TOWARDS DEVELOPMENT OF AN ALGORITHM FOR MAINS WATER TEMPERATURE

Jay Burch and Craig Christensen
National Renewable Energy Laboratory
1617 Cole Blvd.; Golden, CO 80401
E-mail: jay_burch@nrel.gov

ABSTRACT

Mains water temperature (T_{mains}) has significant influence on the energy consumption of water heating equipment. It is dominantly influenced by ambient temperature (T_{amb}). Since T_{amb} is roughly an annual sinusoid, T_{mains} is assumed to be a sinusoid whose mean value varies directly with annual average temperature $T_{amb,ann}$. Model parameters are based on water system physics and include: i) a constant offset from $T_{amb,ann}$; and ii) amplitude and phase which vary linearly with $T_{amb,ann}$. Available T_{mains} data indicate that the offset is ~6 ^oF, and that the amplitude is ~$0.4\Delta T_{amb}$ Uncertainties include: i) data quality issues, including bias of T_{mains} data from heat exchange with house air; ii) inherent spatial variations in mains networks, and iii) limited data sets. Future work includes acquiring quality data sets, testing the model in northern climates, and .refining parameter estimates.

1. INTRODUCTION

Mains water temperature (T_{mains}) is the temperature of the water supplied to the house piping from the water utility's distribution mains piping. T_{mains} affects energy consumption of all water heaters, and its accuracy is of interest. There will be some error (denoted δT_{mains}) in algorithms estimating T_{mains} at any site. δT_{mains} induces a corresponding error in a prediction of water heater energy. For a conventional storage tank water heater (WH) over a period Δt, differentiating the long-term tank energy balance with storage tank losses and manipulating yields:

$$\delta Q_{WH}/Q_{WH} = -[\delta T_{mains}/(T_{set}-T_{mains})][EF_{WH}/\eta_{burn}] \qquad (1)$$

For solar collectors, the temperature difference and incident radiation determine efficiency, as in Fig. 1. δT_{mains} induces an error in the inlet temperature, sliding the operating point along the efficiency curve, as in Fig. 1. Taking differentials of the linear form of the collector efficiency equation yields:

$$\delta\eta_{coll}/\eta_{coll} = - F_rU_l*\delta T_{mains}/(\eta_{coll}I) \qquad (2)$$

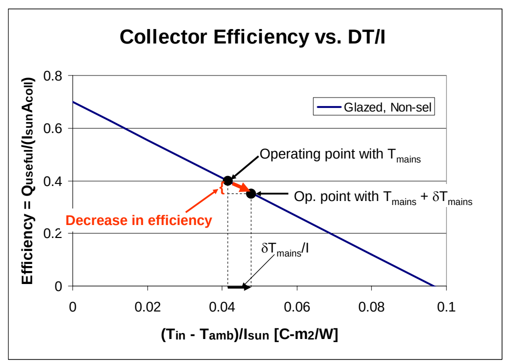

Fig. 1. Collector efficiency plot, showing the decrease in collector efficiency with $\delta T_{mains} > 0$.

Table 1 gives the uncertainty in annual energy calculations for the cases of Eqs. 1,2 with an assumed error of δT_{mains} =+3 ^oC. This value is the difference between the T_{mains} algorithm in (1) and the preliminary algorithm here (Sec. 4). Using values noted in Table 1, errors are 7%-9% in these two simple cases. Although not overwhelmingly large, these errors are large enough to motivate minimizing error in T_{mains} algorithms.

TABLE 1. ANALYSIS SENSITIVITY TO T_{mains}

Analysis Result	Potential Error[1]
Conventional WH annual energy[2]	-7.1%
SWH annual savings[3]	-9.3%

1. Error from Eqs. 1,2, with δT_{mains} = 3 ^oC.
2. T_{set}=50^{o}C;T_{mains}=10^{o}C;EF_{tank}=.95 @V_{draw}=64 gal/day; η_{burn}=0.8.
3. $(F_rU_l)_{coll}$= 5 W/m^{2o}K; I_{avg} = 400 W/m^2; η_{coll}= 0.4.

Previous work <u>in the solar community</u> on T_{mains} has been limited, and the algorithms used in modeling tools have not been well-documented. Existing modeling algorithm types include: i) <u>sinusoid</u> fit to air-temperature data, as in (1); and ii) <u>empirical</u> fit, e.g., expressing $T_{mains,mon}$ as a polynomial in $T_{amb,mon}$ (2). Modeling T_{mains} as a sinusoid with parameters based upon local weather results from recognizing that i) T_{mains} is a strong function of T_{amb}; and ii) T_{amb} is roughly sinusoidal, as shown in Fig. 2. The sinusoid model in (1) calculates T_{mains} as:

$$T_{mains,ref\,(1)} = T_{amb,ann} + R\Delta T_{amb}\sin(\omega_{ann}t - \phi_{amb} - \phi_{mains}) \quad (3)$$

ΔT_{amb} is taken as $[(T_{mon,max} - T_{mon,min})/2]$, and the ratio R is taken as a constant at 0.05. The sinusoid algorithm developed in this study is similar in that T_{mains} has the same direct dependence on local $T_{amb,ann}$ and has amplitude proportional to ΔT_{amb}. The model presented here differs in form from Eqn. 3 by: i) adding in a constant offset (ΔT_{offset}); and ii) expressing R and ϕ_{mains} as linear functions of $T_{amb,ann}$. ΔT_{offset} accounts for factors (such as sun and plant transpiration) which cause the annual average surface temperature to differ from $T_{amb,ann}$. Dependence of R and ϕ on $T_{amb,ann}$ reflects expected consequences of burying pipes deeper in colder climates to prevent freezing.

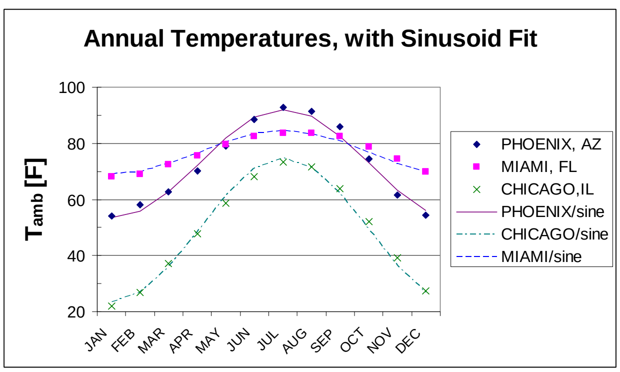

Fig. 2. Monthly air temperature data for three sites, with sine model fits based upon the average and extreme.

2. <u>WATER NETWORKS: GENERAL ISSUES</u>

A block diagram of a potable water supply system is shown in Fig. 3. It is complex, with many factors influencing the water temperature. T_{amb} is a dominant factor, heavily influencing water temperature at all stages of the system, as indicated in Fig. 3. For purposes here, it is useful to break the system into three parts: i) <u>supply</u>, including source, treatment, and storage; ii) <u>mains</u>, the mains distribution line from the storage tank to the house; and iii) <u>house,</u> the piping from mains to the house boundary, and the piping internal to the house. The quantity of interest here is T_{mains}.

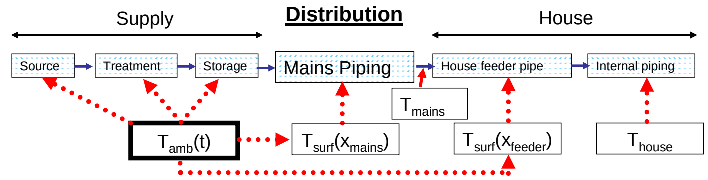

Fig. 3. Block diagram of a potable water supply system, showing importance of T_{amb} on T_{mains}.

2.1 <u>Supply</u>

System water supply comes from surface waters or from well water. Surface waters vary seasonally in temperature, with rivers varying more than lakes/reservoirs. Well water temperature beyond ~30 ft. is constant at the deep-ground temperature, which is close to $T_{amb,ann}$ (3). A local well with "short" piping to the house is a special case of the correlation here, for local wells, the sinusoid expressing annual variation would be dropped. Storage is usually in closed metal tanks exposed to the ambient air. For a well-mixed tank coupled to a constant T_{amb}, the time constant is of order one week, depending on tank size.

2.2 <u>Mains Distribution Piping</u>

The mains distribution piping subjects the water in the pipe to the dynamic influence of ground temperature at the depth to which the pipe is buried ($T_{grd}(z_{pipe},t)$), as in Fig. 4. Mains pipes are typically tens of miles long, and may be a complex maze of interconnecting pipes, valves and pumps, fed by multiple storage tanks supplied from a variety of sources. Modeling temperature in such a complex network would require a vast amount of dynamic information, and direct modeling is considered impractical. Nonetheless, solution of simplified problems may be useful to provide some insight into general features of distribution systems.

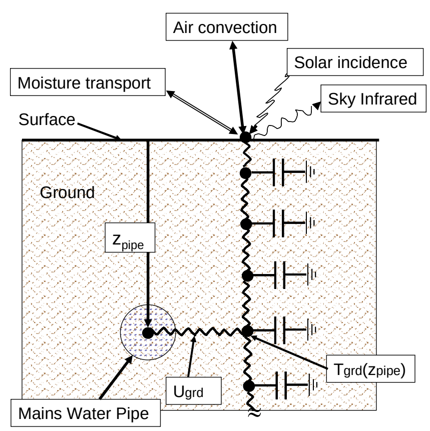

Fig. 4. Buried pipe schematic, with surface energy balance terms and schematic heat transfer model.

2.2.1 Spatial variation in T_{mains}. Generally, T_{mains} is a function of both time and position down the pipe leading from the storage tank, i.e., $T_{mains} = T_{mains}(x_{pipe},t)$. Variation is due to ground interaction and other factors (such as different sources/storage tanks supplying different parts of the network). To illustrate the ground influence, consider the idealized problem of a single pipe at constant depth z_{pipe}, as shown in Fig. 4. Assume $T_{surf}(t)$ is uniform along the pipe length. If the ground capacitance is ignored and assumptions made as in Fig. 4, the temperature along the pipe is given as

$$T_{mains}(x_{pipe})=T_{grd}(z_{pipe})+[T_{mains\text{-}in}-T_{grd}(z_{pipe})]\exp(-x_{pipe}/x_0) \quad (4)$$

where $x_0 = (\rho_{water}c_pD_{pipe}v_{pipe}/4U_{grd})$. Fig. 5 shows x_0 as a function of v_{pipe} for an 8" diameter pipe. Designs will limit $v_{pipe,max}$ to ~3 ft/sec at anticipated peak demand to avoid pipe-wall erosion. However, $v_{pipe,avg}$ might be $1/10^{th}$ that value. At higher velocities and shorter distances, the water will not have come into equilibrium with the ground, and T_{mains} is in between T_{amb} and $T_{grd}(z_{pipe})$. At lower velocities/longer lengths, equilibrium between the water and the ground will be attained, and $T_{mains} = T_{grd}(z_{pipe})$.

Variation in T_{mains} throughout the distribution system is significant. Fig. 6 shows data taken across the metropolitan Denver area over a two-week period in Jan. 2007, a time period near the minimum point in T_{mains} where dT_{main}/dt should be small. The spread is ~10 ^oF. Data in figs. 9d, 9f (at paper's end) show that T_{mains} varies significantly within these two metropolitan areas also. The effect may partly or entirely be due to ground interaction. We conclude that: *a T_{mains} correlation can provide only an average across the water network. For any individual home, T_{mains} may differ from the correlation by up to ± 5 ^oF.*

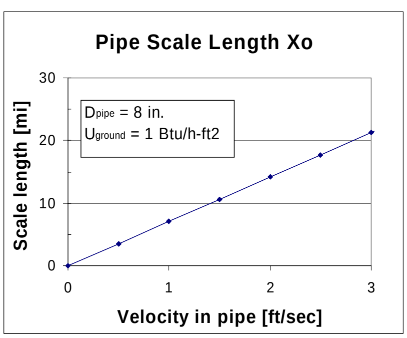

Fig. 5. Scale length x_0 for mains piping as a function of velocity in the pipe. x_o is defined in Eqn. 4; it is the distance where $T_{mains} = T_{grd}(z_{pipe}) + (T_{mains\text{-}in} - T_{grd}(z_{pipe}))/e$.

2.2.2 Ground Temperature. An analytical solution to the ground temperature problem provides guidance for choice of the form of the correlation for T_{mains}. $T_{grd}(z_{pipe},t)$ is determined by the ground surface temperature $T_{surf}(t)$ (3). If $T_{surf}(t)$ is given as a sinusoid [i.e., $T_{surf,ann} + \Delta T_{surf}\sin(\omega_{ann}t - \phi_{amb})$], then solution of the ground conduction boundary value problem (assuming no moisture convection or freeze/thaw occurs) is given by Eqn. 5 (from (3)):

$$T_{grd}(z,t) = T_{surf,ann} + R(z)\Delta T_{surf}\sin(\omega_{ann}t - \phi_{amb} - \phi_{lag}(z)) \quad (5)$$

where: $R(z) = \exp(-z/z_0)$, $z_0 = \sqrt{[2\kappa/\omega_{ann}]}$, $\kappa = k_{grd}/(\rho_{grd}c_{grd})$, and $\phi_{lag}(z) = z/z_0$.

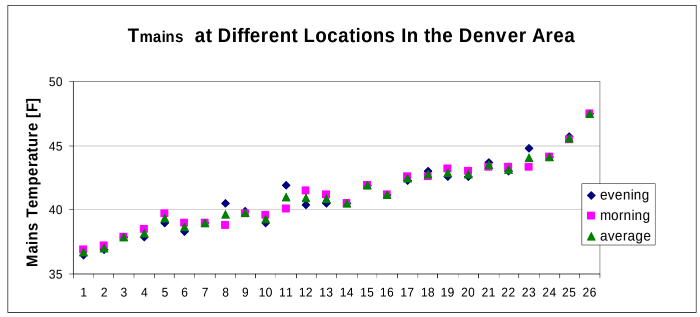

Fig. 6. Mains temperature at different locations in the same area. Data were taken in the Denver Metropolitan area, in mid-Jan. 2007.

Fig. 7 shows $T_{grd}(z_{pipe})$ plots at three depths from Eqn. 5 for Phoenix, Arizona. The curves show the progressive reduction in sinusoid amplitude and increased phase lag as depth increases.

$T_{surf}(t)$ is influenced by a number of factors, as indicated in Fig. 4. It is most strongly coupled with T_{amb}, but is affected by absorbed solar radiation, sky infrared fluxes, rainfall and water percolation, evapotranspiration from plants, snow cover, and freeze-thaw dynamics. In general, we expect

$$T_{surf,ann} = T_{amb,ann} + \Delta T_{offset} \text{ and } \Delta T_{surf} \approx \Delta T_{amb} \quad (6)$$

All the physical drivers but T_{amb} are lumped into the constant ΔT_{offset}. If solar radiation is the largest influence, as expected, we would expect ΔT_{offset} to be positive.

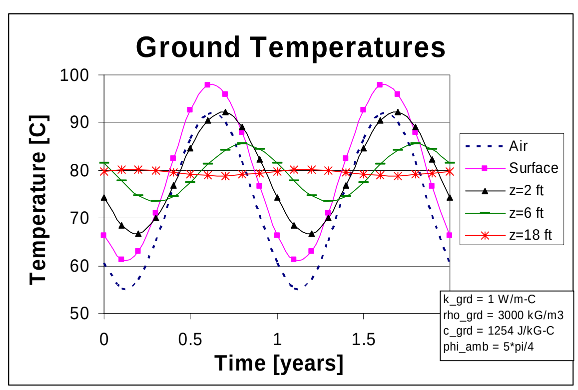

Fig. 7. Plot of $T_{grd}(z,t)$ vs. time for Phoenix, for a 2-year period. T_{amb}, T_{surf}, and T_{grd} at 3 depths are shown.

2.3 House piping

The feeder pipe from the mains to the house boundary may affect T_{mains}, mainly because there may be a very different surface temperature above the feeder pipe (e.g., under a lawn), as opposed to the mains pipe (e.g., under the street). The piping internal to the house generally has a significant affect on the temperature showing up at the end-use points (4), as illustrated in Fig. 8. After a period of several hour with no draws, the water in the house piping will be at temperature T_{house}. As in Fig. 8, the draw-off temperature T_{tap} starts out steady at T_{house}, until a volume of water ~equal to the volume of the upstream piping is drawn. T_{tap} then decays to T_{mains} after draw volume is ~1.5-2.0V_{piping} (4). *For a spot measurement, one should draw at the highest rate possible (e.g., bathtub tap) and wait until the temperature is stable (e.g., 3-5 minutes).* Data in Fig. 6 were ostensibly taken under this protocol.

When using a data-logger, T_{mains} data must be logged conditionally, i.e., data from the T_{mains} sensor reading is taken only when there is a draw. If not, the sensor average is near T_{house} and is meaningless. However, conditional logging still introduces a bias, especially for short draws. If a two minute draw occurs as in Fig. 8 and the data are conditionally averaged over the entire draw, the average T_{draw} value- when interpreted as T_{mains}- is skewed by about 15 ^oF. *With data loggers, one should not accept T_{mains} data until the draw has gone on for 5 min. or so.* It is not known how much this affect contaminates conditionally-logged T_{mains} data from various sources. Note that to accurately estimate the temperature coming into an end-use point (like a water heater), one must model the effect of the pipes between the feeder pipe take-off and the end-use point. Energy to warm or cool the mains water in the house pipes is provided by the house's HVAC systems, trading off with water heater energy. These effects are seldom modeled.

3. T_{mains} CORRELATION

The form of the correlation for $T_{mains}(T_{amb})$ should be a constant + sinusoid, since T_{amb} and T_{surf} are ~sinusoids:

$$T_{mains} = T_{mains,avg} + \Delta T_{mains}\sin(\omega_{ann}t - \phi_{amb} - \phi_{mains}) \qquad (7)$$

It is assumed that T_{amb} is at a minimum on January 15, implying ϕ_{amb} is to be taken as 104.8^o (1.830 rads). The constant term is linear in $T_{amb,avg}$ with an offset similar to that used in Eqn. 6:

$$T_{mains,avg} = T_{amb,avg} + \Delta T_{offset} \qquad (8)$$

ΔT_{mains} and ϕ_{lag} are formulated from trends shown in Eqn. 5. The amplitude in Eqn. 5 is proportional to ΔT_{amb}, and decreases with increasing depth z. Since pipes are buried deeper the colder the climate, we expect R to decrease with decreasing $T_{amb,ann}$. Using a linear function and injecting a reference temperature ($T_{ref} \equiv 44$ ^oF) so that K_1 is the value of R at $T_{amb,ann} = T_{ref}$, one has:

$$\Delta T_{mains} = R\Delta T_{amb} = [K_1 + K_2(T_{amb,ann} - T_{ref})]\Delta T_{amb} \qquad (9)$$

Similarly, the phase lag ϕ_{mains} is expected to increase with increased z_{pipe}, as in Eqn. 5 and Fig. 7, and a similar linear expression for ϕ_{mains} is proposed (expecting $K_4 < 0$):

$$\phi_{lag} = K_3 + K_4(T_{amb,ann} - T_{ref}) \qquad (10)$$

ΔT_{offset} and $\{K_i, i=1,4\}$ are parameters to be determined by fitting to data sets for T_{mains} spanning a wide range of $T_{amb,ann}$.

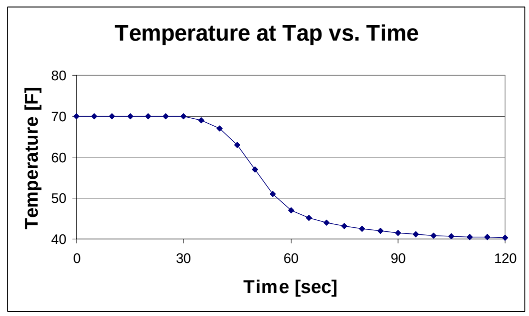

Fig. 8. Temperature at a cold water tap with draw, given no previous draw for several hours. After purging the upstream pipe volume, the tap outlet temperature transitions from T_{house} (~70 ^oF) to T_{mains} (~40 ^oF).

There is a practical difficulty in determining the values for the T_{amb} variables in Eqn. 7-10, because T_{amb} data should be coincident with the T_{mains} data. Ideally, T_{mains} data sets should provide $T_{amb}(t)$, overlapping the T_{mains} data (and also ideally extending back in time for a year or so). If average weather like TMY2 (5) is used for calculating T_{amb} values, a random error equal to the RMS variation of annual average temperature (~1 ^oC) is introduced. Data from other sources such as (6) could be used to get coincident T_{amb} data if not available from the data set directly.

4. DATA SETS AND CORRELATION COEFFICIENTS

Data sets used in this study are shown in Figs. 9a-9i (from (2), (7), and (8)). Local well-water sites in (7) were identified based upon T_{mains} being ~constant and were removed from the analysis. TMY2 data (5) was used for T_{amb} in all cases. The model results are also shown in Figs 9-17. The parameters of the model for the fit shown here are given in Table 2. RMS error between model and data across the sites in Figs. 9a-9i is ~4 °F. The model for the coldest climate (Fig. 9a, Duluth Minnesota) is low by ~13 °F. This may indicate affects of freeze-thaw or snow cover (which invalidate the simple ground model used in Sec. 2). However, other northern sites do not show similar poor fits. Otherwise, the model-data discrepancies are small, usually within 5 °F or so. Variation of R and ϕ_{lag} with $T_{amb,ann}$ is shown in Fig. 10. The ratio R ranges from ~0.35 (coldest) to ~0.7 (hottest) across the continental U.S. Similarly, the phase lag ϕ_{mains} ranges from about ~10° (hottest) to ~40° (coldest).

TABLE 2. PARAMETERS FOR T_{mains} CORRELATION

Parameter	Value
ΔT_{offset}	6.0 °F
K_1	0.4
K_2	+0.010 $°F^{-1}$
K_3	35 Deg
K_4	-0.01 Deg/°F

5. CONCLUSIONS AND FUTURE WORK

Results in common water heating analyses depend on T_{mains}, and typical uncertainty/error in T_{mains} can lead to ~10% error in calculations. Data show that T_{mains} varies along the distribution network by ±5 °F, implying that any simple T_{mains} algorithm can provide only an average value. From general consideration of water systems, it is concluded T_{mains} is heavily influenced by T_{amb}, which is sinusoidal. A sinusoidal correlation linear in $T_{amb,ann}$ is proposed, introducing several new parameters. The average value of T_{mains} is $T_{amb,ann}$ plus an offset $\Delta T_{offset} \approx 6$ °F. The amplitude is given as $R\Delta T_{amb}$, with $R \approx 0.4$ and R decreasing linearly with decreasing $T_{amb,ann}$. The phase lag between T_{mains} and T_{amb} decreases linearly with increasing $T_{amb,avg}$. Data from 9 areas in the U.S. were used to determine coefficients. It is not known if the data are biased by residual influence of T_{house} on T_{mains} data, but it is likely that is the case. This would show up as an increase in ΔT_{offset} (i.e., bias in the T mains algorithm). Additional data are being sought to test the algorithm form and reduce error in parameter estimates. The algorithm form may need to be modified for cold climates where ground freeze and snow cover exist in winter-time.

6. ACKNOWLEDGMENTS

The authors acknowledge funding from the U.S. Department of Energy's Solar Energy Technology Program, Solar Heating and Lighting (SH&L) sub-program, managed by Tex Wilkins and Glenn Strahs.

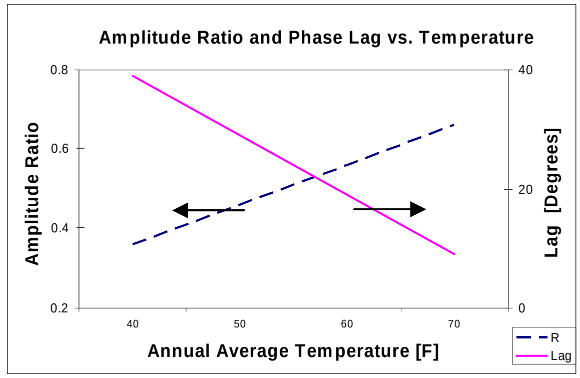

Fig. 10. Amplitude ratio R and phase lag ϕ_{lag} vs. $T_{amb,ann}$.

7. NOMENCLATURE

Symbols

A	Area of collector
c_p	Heat capacity at constant pressure
D	Pipe diameter
e	natural logarithms base, ~2.72
EF	Energy factor of tank ($Q_{to\text{-}load}/Q_{energy\text{-}in}$)
F_r	Heat removal factor in collector theory
k	Conductivity of soil
K	Constant in T_{mains} correlation
I	Solar irradiance in the plane of the collector
M	Mass (of water)
Q	Energy
R	Ratio of amplitudes, $\Delta T_{grd}(z)/\Delta T_{surf}$
t	Time
T	Temperature
U	Loss coefficient
V	Volume contained in piping
x	Horizontal distance down the mains pipe
x_0	Scale length (1/e distance)
z	Vertical distance down from ground surface
z_0	Scale length for temperature decay (1/e distance)
Δ	Amplitude or difference
κ	$k/\rho c$
η	Efficiency (collector or fuel conversion)
ρ	Density
ω	Angular frequency

Subscripts

amb	Ambient air dry bulb temperature
ann	Annual time period (one year period)
avg	Average value
burn	burner (for gas water heaters)
coll	Collector
i	Index for data points or correlation parameters
in	Inlet to pipe or end use
mains	Water in the mains distribution piping
mon	Month time period

offset ΔT shift from $T_{amb,ann}$ in T_{mains} correlation
pipe Mains distribution or house internal piping
ref Reference temperature, ~ U.S. average
set Set-point temperature of water heater
tap End-use point in the house
WH Water heater

8. REFERENCES

(1) Private Communication, Dr. Sandy Klein, Solar Energy Laboratory, Madison, WI. The algorithm is used in FCHART, a well-known solar program. However, it is not documented anywhere, to our knowledge.

(2) Private communication from Danny Parker, Florida Solar Energy Center, Cocoa Beach, FL.

(3) Carslaw, H. and Jaeger, J., Conduction of Heat in Solids, 2nd Edition, 1959. University Press, Oxford, U.K.

(4) Wendt, R., Baskin, E., and Durbin, D. "Evaluation of Hot Water Distribution Systems by Numeric Simulation", Final Report, Energy Commission Contract No: 400-00-038. March 2004.

(5) TMY2 data sets are described and available at: http://rredc.nrel.gov/solar/old_data/nsrdb/tmy2/

(6) National Climatic Data Center, Asheville, North Carolina.

(7) Abrams, D., and Shedd, A., "Effect of Seasonal Changes in Use Patterns and Cold Water Inlet Temperature on Water-Heating Loads", 1996. ASHRAE Transactions, 1986.

(8) Private communication from Tim Moss, Sandia National Laboratory, Albuquerque, NM.

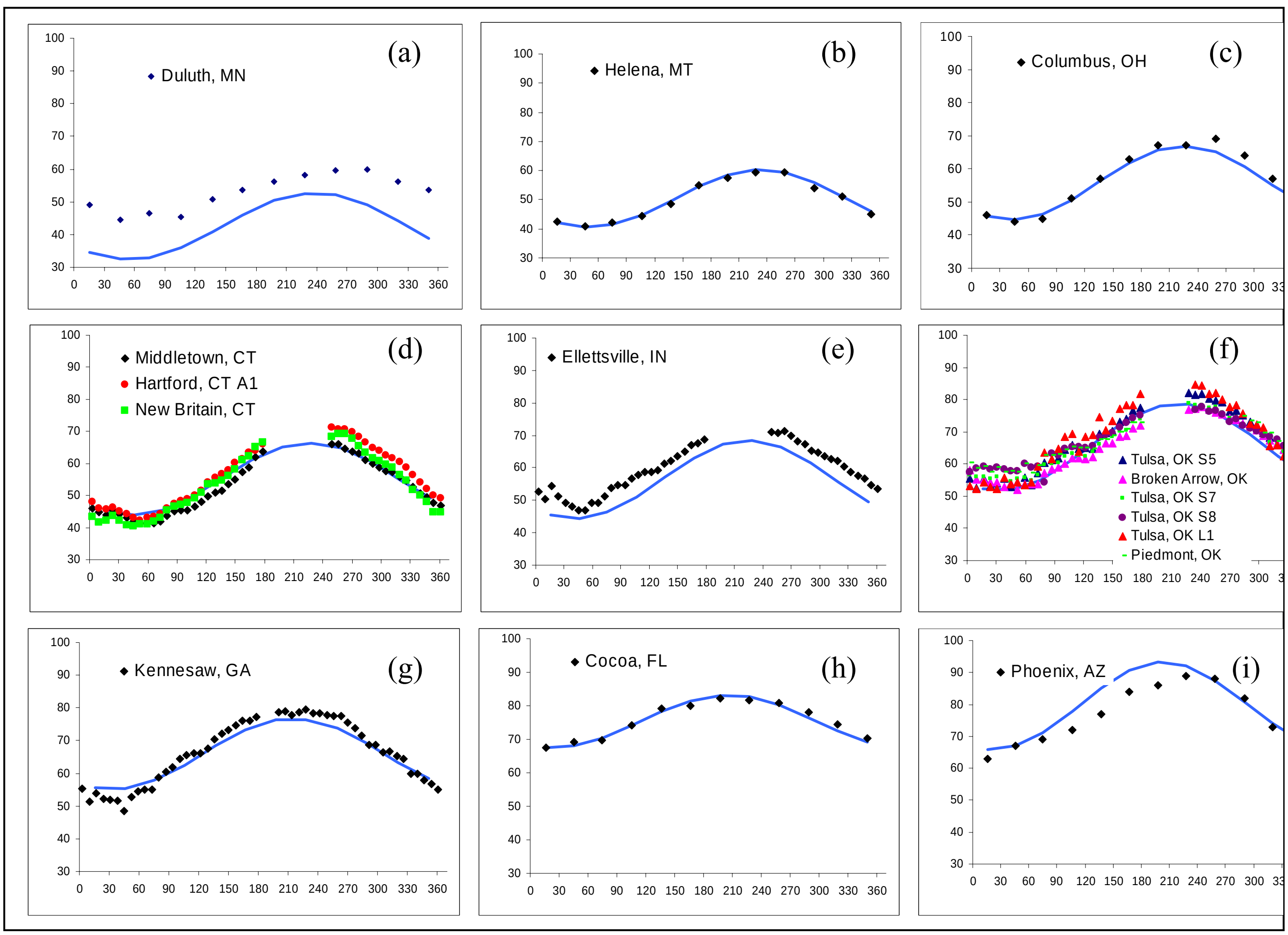

Figs. 9a-9i. T_{mains} data over a year for 9 U.S. locations, with Julian Day on the x axis, and T_{mains} on the y axis, for all plots. Data are shown as symbols, and the T_{mains} correlation result is the blue curve, using TMY2 data to calculate the T_{amb} terms in Eqs. 7-10.